Fabrication and Performance of Selectively Oxidized Vertical-Cavity Lasers

Kent D. Choquette, K. L. Lear, R. P. Schneider, Jr., K. M. Geib, J. J. Figiel, and Robert Hull

Abstract— We report the high yield fabrication and reproducible performance of selectively oxidized vertical-cavity surface emitting lasers. We show that linear oxidation rates of AlGaAs without an induction period allows reproducible fabrication of buried oxide current apertures within monolithic distributed Bragg reflectors. The oxide layers do not induce obvious crystalline defects, and continuous wave operation in excess of 650 h has been obtained. The high yield fabrication enables relatively high laser performance over a wide wavelength span. We observe submilliamp threshold currents over a wavelength range of up to 75 nm, and power conversion efficiencies at 1 mW output power of greater than 20% over a 50-nm wavelength range.

Fig. 1. Sketch of an oxide-confined VCSEL showing oxidized layers and the resulting current apertures on each side of the optical cavity.

WET OXIDATION of AlGaAs [1], [2] has been successfully employed in the fabrication of edge emitting lasers, [3] and has recently been applied to various vertical-cavity surface emitting laser (VCSEL) diode structures [4]–[9]. For example, VCSEL's incorporating GaAs–Al-oxide layers for high-index contrast distributed Bragg reflector (DBR) mirrors have been reported [4]. Partial oxidation of AlAs layers in the DBR mirror stack has been pursued to form a high-index cladding around the laser cavity [5]. Finally, using oxide layers to form current apertures under hybrid dielectric DBR's [6] or monolithic semiconductor DBR's [7] has also been demonstrated. The latter oxide-confined lasers have exhibited the highest power conversion efficiency (>50%), [8] lowest threshold current density (90 A/cm^2 per quantum well), [9] and lowest threshold voltage (50 mV above photon energy) [7] reported to date for VCSEL's. In this letter we report on the high-yield fabrication and reproducible performance of monolithic selectively oxidized VCSEL's. As opposed to record operation, we show that samples of large arrays of these lasers also exhibit relatively high performance levels over a wide lasing wavelength span that may be attractive for emerging VCSEL applications.

Fig. 1 is a schematic of our top-emitting VCSEL, which employs selective oxidation to produce buried oxide current apertures [7]. This oxide-confined VCSEL has several advantages. First, in this monolithic structure we fully exploit low resistance p-type DBR designs (such as parabolic heterointer-
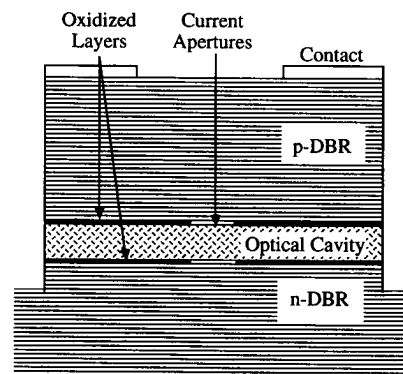
face grading [10] and C-doping [11]) in utilizing the entire top mirror to conduct current into the active region. Thus, current crowding effects of thin intracavity contact layers [6] or ion implantation damage in the top DBR are both avoided. The current apertures immediately surrounding the optical cavity also eliminate sidewall nonradiative recombination present in etched air-post VCSEL's [12], and minimize lateral current spreading to outside of the laser cavity. Finally, the smaller refractive index of the Al–oxide layer [13] also induces index-guided optical confinement [14], [15], but in a planar VCSEL configuration amenable to efficient current flow and heat extraction. Comparing oxide-confined VCSEL's to ion implantation-defined VCSEL's, the enhanced electrical and optical confinement of the former produces reduced threshold current/voltage and the concomitant parasitic ohmic heating [9]. In the following, we describe the properties of 980 nm VCSEL's, although similar 850 and 650 nm [16] oxide-confined lasers have also been characterized.

The two-inch diameter VCSEL wafers are grown by metalorganic vapor phase epitaxy on a rotating susceptor, and have three InGaAs quantum wells in the active region. The monolithic DBR mirrors consist of GaAs–Al$_{0.92}$Ga$_{0.08}$As layers with parabolic heterointerface grading. The low index layers adjacent to the optical cavity are adjusted to Al$_{0.98}$Ga$_{0.02}$As to increase their oxidation rates relative to the other DBR layers [7]. Fabrication of oxide-confined VCSEL's begins with the lift-off deposition of a top Ti–Pt–Au contact. A nitride mask is then deposited and patterned to encapsulate the metal contact and form a mesa etch mask. Reactive ion etching with BCl$_3$–Cl$_2$ is used to define the mesas and expose the sidewalls for oxidation. The samples are oxidized at 450 °C under flowing nitrogen, which is bubbled through water at
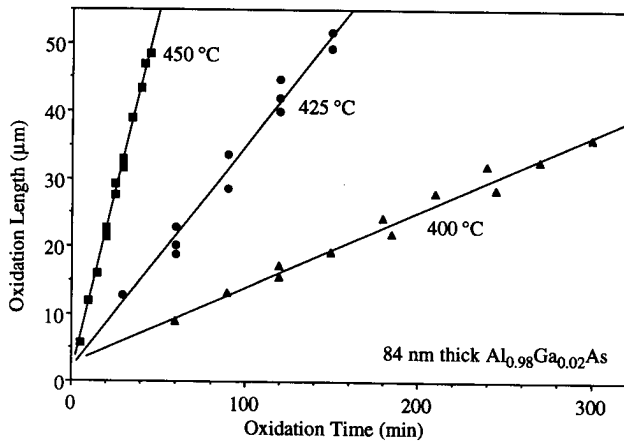
Fig. 2. Lateral extent of oxidation at 400, 425, and 450 °C for a 84-nm-thick $Al_{0.98}Ga_{0.02}As$ layer contained within a distributed Bragg reflector, showing linear oxidation rates without induction periods.

Fig. 3. Cross-section transmission electron micrograph ($g = (311)$ bright field image) of a selectively oxidized VCSEL showing the oxide layer above the quantum-well (QW) active region. The dark (light) layers in the DBR mirror are GaAs (AlGaAs). The terminus of the buried oxide layer, which forms the perimeter of the current aperture, is at the vertical arrow.

85 °C. After oxidation the nitride mask is removed and a backside Ge–Au–Ni–Au contact is deposited and annealed. In this work we fabricate repeating rows of square mesas that vary in size from 48–90 μm on a side. Oxidation conditions are selected to give an oxide penetration length of 24 μm to "pinch off" the smallest mesa, thus producing arrays of VCSEL's with current apertures of 2×2 μm and larger. For each wafer examined, multiple samples are processed under similar oxidation conditions, where each sample extends from the wafer center to the edge.

To develop reproducible oxidation processes, test samples have been oxidized using different Al compositions, furnace temperatures and oxidation times. The extent of the lateral oxidation of a buried 84-nm-thick $Al_{0.98}Ga_{0.02}As$ layer within a DBR mirror is plotted in Fig. 2. Fig. 2 shows that the lateral oxidation has a temperature dependent linear oxidation rate without an induction time preceding the onset of oxidation. Hence, reproducible fabrication of oxide apertures can be achieved on similar samples from a given wafer. However, the oxidation rate of $Al_xGa_{1-x}As$ is very sensitive to Al composition, where x varying from 1–0.82 changes the relative oxidation rate by more than two orders of magnitude [7]. Thus, the scatter of the oxidation rates in Fig. 2 may be partially related to small composition variations between the test samples. For example, near the edge of a wafer the oxidation rate is consistently found to monotonically decrease, presumably reflecting a slight increase of the Ga content arising from a growth edge effect. In addition, nominally identical wafers may have oxidation rates (at the center) that differ by $\approx$10%. Therefore, stringent compositional control may be necessary for wafer scale manufacture of uniformly sized oxide apertures.

A cross-section transmission electron micrograph of a selectively oxidized VCSEL is shown in Fig. 3. The rounded terminus of the oxide layer in the top mirror is denoted at the vertical arrow in Fig. 3; the unoxidized region beyond this point corresponds to the interior of the current aperture which defines the laser cavity. In Fig. 3, and all other samples that have been examined by transmission electron microscopy, no dislocations or other crystalline defects are apparent along
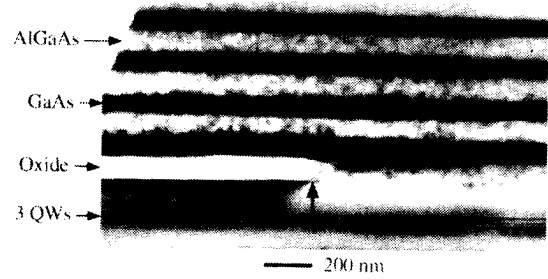
the oxide/semiconductor interface or near the oxidation terminus. Hence, the formation of the oxide layer does not induce obvious defects which would lead to degraded VCSEL operation or lifetime. This is consistent with our observation of approximately 98% yield of all oxide-confined VCSEL's tested to date. Moreover, the first lifetime experiment from a randomly chosen VCSEL has shown unchanged characteristics during >650 hours of CW operation at room temperature (7 mA constant current producing 1.1 mW output light) on a probe station.

In Fig. 4, we plot the threshold current, I_{th}, of VCSEL's from two wafers grown more than a month apart with the same epitaxial structure, which utilizes relatively high reflectivity top mirrors. The data points in Fig. 4 correspond to lasers that are spatially separated by 1 mm, showing that both I_{th} and threshold wavelength vary radially, that latter due to thickness nonuniformity of the VCSEL wafers. The I_{th} wavelength variation arises from the spectral mismatch between the cavity resonance and the laser gain. The minimum I_{th} occurs at $\approx$970 nm, corresponding to the optimal overlap of cavity resonance/peak gain. Notice I_{th} around this wavelength are relatively insensitive to the lasing wavelength. Specifically over the wavelength span of 945–980 nm, the average threshold current is 292μA $\pm$ 6.5% for 5 × 5-μm VCSEL's in wafer XF114, and is 360 μA $\pm$ 5.3% for 7 × 7-μm VCSEL's in wafer XF225. For comparison, implanted VCSEL's (15 μm diameter) fabricated from wafer XF114 have an average threshold current of 4.4 mA $\pm$ 10% over the same wavelength span of 945–980 nm. All of the oxide-confined VCSEL's in Fig. 4 have threshold currents less than 1 mA, corresponding to an operating wavelength span of up to 75 nm. The maximum output power for the VCSEL's in Fig. 4 vary from 0.5–1.5 mW, in spite of the relatively high output coupler reflectivity. Fig. 4 illustrates that submilliamp I_{th} can be reproducibly obtained from oxide-confined VCSEL's.

Fig. 5 depicts the power conversion (wall plug) efficiency obtained at 1-mW output power from VCSEL's fabricated from two other wafers. The lasers in Fig. 5 have reduced output coupler reflectivity where wafer XF130C has a single current aperture in the p-type DBR, and wafer XF130B has double apertures, as depicted in Fig. 1. For these wafers the highest efficiency again occurs at $\approx$ 970 nm. The highest efficiency measured was 30%, where the maximum typically
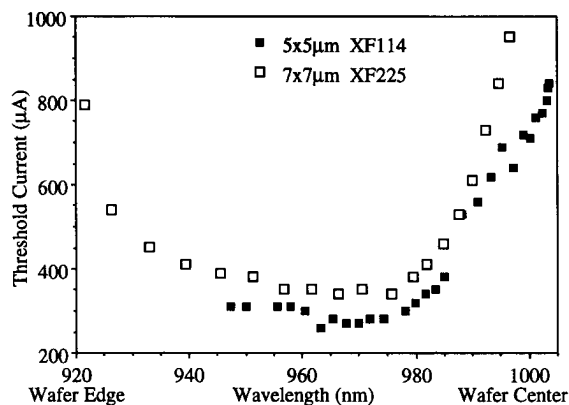
Fig. 4. Threshold current versus threshold wavelength at room temperature for oxide-confined VCSEL's from two wafers. The lasers in wafer XF114 (XF225) have 5 × 5-μm (7 × 7-μm) sized current apertures.
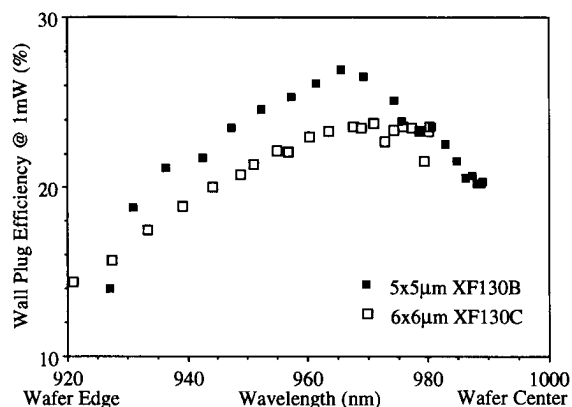

Fig. 5. Wall-plug efficiency at 1-mW output power at room temperature for oxide-confined VCSEL's. The lasers in wafer XF130B have a single 5 × 5-μm sized current aperture, while VCSEL's in wafer XF130C have two 6 × 6-μm-sized current apertures surrounding the optical cavity.

occured between 1–3 mW output power. As shown in Fig. 5 at 1-mW output power, greater than 20% efficiency is obtained over more than a 50-nm wavelength range for wafer XF130B, and similar results are found from wafer XF130C (note the center resonance wavelength of this wafer is shorter). Over this wavelength range I_{th} varies from 0.8–1.4 mA for VCSEL's from both wafers. Since 1 mW output is appropriate for many VCSEL applications, achieving high efficiency at this power is desirable. Maintaining wavelength insensitive I_{th} and wall plug efficiency will impart higher yield to specification for VCSEL arrays in the presence of wafer nonuniformity.

In conclusion, monolithic oxide-confined VCSEL's not only demonstrate benchmark performance records, they also exhibit reproducible and wavelength insensitive performance levels which are attractive for potential applications. We have developed a reproducible and high yield selective oxidation process for fabrication of robust oxide-confined VCSEL's. Moreover, selectively oxidized VCSEL's have been fabricated at emission wavelengths of 980, 850, and 650 nm, which indicates the universality of this VCSEL structure. High-performance oxide-confined VCSEL's, appropriate for a variety of wavelengths, should benefit emerging applications and markets considered for VCSEL's.

ACKNOWLEDGMENT

REFERENCES

[1] W. T. Tsang, "Self-terminating thermal oxidation of AlAs epilayers grown on GaAs by molecular beam epitaxy," *Appl. Phys. Lett.*, vol. 33, pp. 426–429, 1978.

[2] J. M. Dallesasse, N. Holonyak, Jr., A. R. Sugg, T. A. Richard, and N. El-Zein, "Hydrolyzation oxidation of $Al_xGa_{1-x}As$–AlAs–GaAs quantum well heterostructures and superlattices," *Appl. Phys. Lett.*, vol. 57, pp. 2844–2846, 1990.

[3] J. M. Dallesasse and N. Holonyak, Jr., "Native-oxide stripe-geometry $Al_xGa_{1-x}As$–GaAs quantum well heterostructure lasers," *Appl. Phys. Lett.*, vol. 58, pp. 394–396, 1991.

[4] M. H. MacDougal, P. D. Dapkus, V. Pudikov, H. Zhao, and G. M. Yang, "Ultralow threshold current vertical-cavity surface emitting lasers with AlAs–oxide–GaAs distributed Bragg reflectors," *IEEE Photon. Technol. Lett.*, vol. 7, pp. 229–231, 1995.

[5] Y. Hayashi, T. Mukaihara, N. Hatori, N. Ohnoki, A. Matsutani, F. Koyama, and K. Iga, "Record low threshold index-guided InGaAs/AlGaAs vertical-cavity surface emitting laser with a native oxide confinement structure," *Electron. Lett.*, vol. 31, pp. 560–561, 1995.

[6] D. L. Huffaker, D. G. Deppe, K. Kumar, and T. J. Rogers, "Native-oxide defined ring contact for low threshold vertical-cavity lasers," *Appl. Phys. Lett.*, vol. 65, pp. 97–99, 1994.

[7] K. D. Choquette, R. P. Schneider, Jr., K. L. Lear, and K. M. Geib, "Low threshold voltage vertical-cavity lasers fabricated by selective oxidation," *Electron. Lett.*, vol. 30, pp. 2043–2044, 1994.

[8] K. L. Lear, K. D. Choquette, R. P. Schneider, Jr., S. P. Kilcoyne, and K. M. Geib, "Selectively oxidized vertical-cavity surface emitting lasers with 50% power conversion efficiency," *Electron. Lett.*, vol. 31, pp. 208–209, 1995.

[9] K. D. Choquette, K. L. Lear, R. P. Schneider, Jr., and K. M. Geib, "Cavity characteristics of selectively oxidized vertical-cavity lasers," *Appl. Phys. Lett.*, vol. 66, pp. 3413–3415, 1995.

[10] R. P. Schneider, Jr., J. A. Lott, M. Hagerott Crawford, and K. D. Choquette, "Epitaxial design and performance of AlGaInP red (650–690 nm) VCSEL's," *Inter. J. High Speed Electron. and Syst.*, vol. 5, pp. 625–666, 1994.

[11] K. L. Lear, R. P. Schneider, Jr., K. D. Choquette, S. P. Kilcoyne, J. J. Figiel, and J. C. Zolper, "Vertical-cavity surface emitting lasers with 21% efficiency by metalorganic vapor phase epitaxy," *IEEE Photon. Technol. Lett.*, vol. 6, pp. 1053–1055, 1994.

[12] K. D. Choquette, G. Hasnain, Y. H. Wang, J. D. Wynn, R. S. Freund, A. Y. Cho, and R. E. Leibenguth, "GaAs vertical-cavity surface emitting lasers fabricated by reactive ion etching," *IEEE Photon. Technol. Lett.*, vol. 3, pp. 859–862, 1991.

[13] F. A. Kish, S. J. Caracci, N. Holonyak, Jr., J. M. Dallesasse, K. C. Hsieh, M. J. Ries, S. C. Smith, and R. D. Burnham, "Planar native-oxide index-guided $Al_xGa_{1-x}As$ quantum well heterostructure lasers," *Appl. Phys. Lett.*, vol. 59, pp. 1755–1757, 1991.

[14] D. L. Huffaker, J. Shin, and D. G. Deppe, "Lasing characteristics of low threshold microcavity lasers using half-wave spacer layers and lateral index confinement," *Appl. Phys. Lett.*, vol. 66, pp. 1723–1725, 1995.

[15] K. L. Lear, K. D. Choquette, R. P. Schneider, Jr., and S. P. Kilcoyne, "Modal analysis of a small surface emitting laser with a selectively oxidized waveguide," *Appl. Phys. Lett.*, vol. 66, pp. 2616–2618, 1995.

[16] K. D. Choquette, R. P. Schneider, Jr., M. H. Crawford, K. M. Geib, and J. J. Figiel, "Continuous wave operation of 640–660 nm selectively oxidized AlGaInP vertical-cavity lasers," *Electron. Lett.*, vol. 31, pp. 1145–1146, 1995.